

# Emergent new symmetry from the Higgs shadow

Waleed Abdallah,<sup>1,\*</sup> Anjan Kumar Barik,<sup>2,†</sup> Santosh Kumar Rai,<sup>2,‡</sup> and Tousik Samui<sup>2,§</sup>

<sup>1</sup>*Department of Mathematics, Faculty of Science, Cairo University, Giza 12613, Egypt*

<sup>2</sup>*Regional Centre for Accelerator-based Particle Physics, Harish-Chandra Research Institute, HBNI, Chhatnag Road, Jhansi, Prayagraj (Allahabad) 211019, India*

We show in this Letter how a new hidden gauge symmetry responsible for neutrino mass as well as dark matter (DM) in the Universe can be discovered through scalar mediators responsible for breaking the new symmetry. The new force mediator ( $Z'$ ) may be lighter than the Standard Model (SM) gauge bosons but cannot be observed in traditional searches for new gauge bosons. We highlight a novel way of discovering such a symmetry at the Large Hadron Collider (LHC) by incorporating an existing ATLAS analysis on four lepton final states which include the Higgs resonance. In addition, we show that the hidden sector also introduces flavor violation in the lepton sector which can become a significant channel of discovery for the new force.

While the new century welcomed the discovery of a 125 GeV scalar [1, 2] which completes the Standard Model (SM) picture of observed particle spectrum, it also opened up the realm of the unknown structure beyond the SM. Despite the remarkable success of SM, several unexplained observations from experiments, be it neutrino mass or the existence of dark matter (DM), have always hinted at the possibility of new physics beyond the SM (BSM). However the sole discovery of the Higgs boson and nothing else at the Large Hadron Collider (LHC) has cast a shadow on what that exact possibility may be. The non-observation of any new physics signal could be due to the presence of very weakly interacting particles (defined by a symmetry that remains hidden in the LHC data) which may emerge in channels yet to be looked at by the experiments. In this Letter, we highlight that such a new symmetry may be lurking under the shadow of the most important discovery of the current century in particle physics, *viz.* the Higgs boson. We also show that this symmetry can provide a solution to both the neutrino mass problem as well as DM signals.

The importance of  $U(1)$  symmetries have been significantly emphasized in new BSM ideas [3–11] spanning neutrino physics, cosmology, DM, extra dimensions, and supersymmetry, to name a few. They not only provide remedies to several outstanding issues in model building, but also manifest in our understanding of nature via several conserved global symmetries [12, 13]. The hope of observing such a symmetry in experiments has seen a continuous effort over the last few decades at energy scales spanning a few MeV to several TeV. Our proposal of a hidden symmetry tries to present a novelty to the natural extension of the SM by a  $U(1)$  gauge symmetry, by connecting the visible world with the *missing* (neutrinos and DM) while simultaneously suggesting why new physics still remains elusive to us at experiments like the LHC. We propose a neutrinophilic  $U(1)_X$  extension [14, 15] to the SM where any direct signal of the new symmetry is dependent on its overlap with SM particles. We have studied this model [14] in an earlier work featuring multi-lepton signals at the LHC through

heavy neutrino production. A crucial part in that analysis was played by the non-vanishing gauge kinetic mixing (GKM) of the SM  $U(1)_Y$  with the new  $U(1)_X$  symmetry. In the absence of any meaningful mixing of  $Z'$  with the  $Z$  boson, we highlight an interesting signal that would be able to probe the new  $Z'$  directly via Higgs production and provide a robust signal in the current LHC run. As the  $U(1)_X$  symmetry is broken by a singlet scalar, its admixture in the observed scalar at the LHC allows the  $Z'$  to couple with the SM-like Higgs boson. A similar production mechanism in the context of  $U(1)_{B-L}$  for  $Z'$  was considered in Refs. [16, 17]. However, to obtain a light  $Z'$  in that model and to avoid LHC constraints, the gauge coupling  $g_{B-L}$  is restricted to unnaturally small values. This makes the contribution coming from the second scalar insignificant. In our case, the new gauge coupling ( $g_x$ ) remains naturally large with  $g_x \sim g_2 \sim g_1$ , where  $g_1, g_2$  are coupling strengths for  $U(1)_Y$  and  $SU(2)_L$  gauge symmetries, respectively. We find that this gives a larger production rate for the  $Z'$  through an additional scalar.

An additional phenomenologically interesting scenario occurs when the GKM vanishes completely. Then the  $Z'$  in the model can become dominantly leptophilic. This happens when the decay of the  $Z'$  is driven by one-loop contributions over the tree-level mode. An interesting outcome of the one-loop driven decay of the  $Z'$  is lepton flavor violations (LFV) that could lead to interesting signatures of the new symmetry. The lightest of the heavy SM singlet neutrino of the model can also contribute to the cold dark matter (DM), since the light  $Z'$  provides a new channel for a sufficient amount of neutrino annihilation into  $Z'$  pair. Thus one can summarise several interesting possibilities in a common framework:

- A light sub-100 GeV  $Z'$  signal at the LHC via Higgs production.
- A compatible fermionic DM with the correct relic density ensured by the presence of the light  $Z'$ .
- Neutrino mass generation via inverse-seesaw mech-

| Fields      | $SU(3)_C$ | $SU(2)_L$ | $U(1)_Y$ | $U(1)_X$ | Spin  |
|-------------|-----------|-----------|----------|----------|-------|
| $H_{1(2)}$  | 1         | 2         | $-1/2$   | $0 (-1)$ | 0     |
| $S$         | 1         | 1         | 0        | 2        | 0     |
| $N_{L/R}^i$ | 1         | 1         | 0        | 1        | $1/2$ |

TABLE I. New scalars ( $H_1, H_2, S$ ) and matter fields ( $N_L^i, N_R^i, i = 1, 2, 3$ ) and their charge assignments under the SM gauge group and  $U(1)_X$ .

anism [14]<sup>1</sup>.

- Lepton flavor violating (LFV) signal at one-loop through  $Z'$  decay and possible contribution to lepton anomalous magnetic moments.

The model is an extension of the SM with an extra  $U(1)_X$  gauge group and four new fields, including two chiral sterile neutrinos  $N_L, N_R$  added for each generation, an additional Higgs doublet  $H_2$  and a scalar singlet  $S$ , where all the new fields are charged under  $U(1)_X$  while all SM particles are neutral. The charge assignments of the new particles along with the first Higgs doublet ( $H_1$ ) are listed in Table I. The new scalar doublet ensures that a Dirac mass term for the neutrinos, necessary for the inverse-seesaw mechanism, is guaranteed. All the new fields are charged under  $U(1)_X$  while all SM particles are neutral. The new charge-neutral fermions mix with the SM neutrinos after symmetry breaking. With the assigned charges, the new gauge invariant Lagrangian added to the SM is given by (neglecting the kinetic terms)

$$\begin{aligned}
\mathcal{L}_S &\supset -\mu_1 H_1^\dagger H_1 - \mu_2 H_2^\dagger H_2 - \mu_s S^\dagger S + \{\mu_{12} H_1^\dagger H_2 + \text{h.c.}\} \\
&\quad - \lambda_1 (H_1^\dagger H_1)^2 - \lambda_2 (H_2^\dagger H_2)^2 - \lambda_s (S^\dagger S)^2 - \lambda'_{12} \left| H_1^\dagger H_2 \right|^2 \\
&\quad - \lambda_{12} H_1^\dagger H_1 H_2^\dagger H_2 - \lambda_{1s} H_1^\dagger H_1 S^\dagger S - \lambda_{2s} H_2^\dagger H_2 S^\dagger S, \\
\mathcal{L}_Y &\supset -\{Y_\nu \bar{l}_L H_2 N_R + Y_R S \bar{N}_R N_R^C + Y_L S \bar{N}_L N_L^C + \text{h.c.}\}, \\
\mathcal{L}_M &\supset -\hat{M}_N (\bar{N}_L N_R + \bar{N}_R N_L). \tag{1}
\end{aligned}$$

We refer the readers to Ref. [14] for more details on the model and its parameters, which lead to the masses and mixings of the fermions, scalars and gauge bosons. Note that  $\mu_{12}$  is the coefficient of a soft-breaking term<sup>2</sup> which breaks the  $U(1)_X$  symmetry explicitly. Such a term can have its origin in a larger symmetry sitting at a much higher energy scale [18].

After spontaneous breaking of the electroweak (EW) and  $U(1)_X$  symmetries when  $H_{1/2}$  and  $S$  acquire VEVs, we are left with three physical CP-even neutral Higgs

bosons, a charged Higgs and a pseudoscalar Higgs. The CP-even scalar mass matrix in the  $(\rho_1 \ \rho_2 \ \rho_3)^T$  basis [14] is

$$M_H^2 = \begin{pmatrix} 2\lambda_1 v_1^2 + \mu_{12} \frac{v_2}{v_1} & \Lambda_{12} & \lambda_{1s} v_1 v_s \\ \Lambda_{12} & 2\lambda_2 v_2^2 + \mu_{12} \frac{v_1}{v_2} & \lambda_{2s} v_2 v_s \\ \lambda_{1s} v_1 v_s & \lambda_{2s} v_2 v_s & 2\lambda_s v_s^2 \end{pmatrix}, \tag{2}$$

where  $\Lambda_{12} = (\lambda_{12} + \lambda'_{12})v_1 v_2 - \mu_{12}$  and  $v_{1(2)}$  is the vacuum expectation value (VEV) of  $H_{1(2)}$ . The three CP-even mass eigenstates ( $h_1, h_2$  and  $h_3$ ) are linear combinations of the flavor states ( $\rho_i$ ) via the mixing matrix  $Z^h$ , i.e.  $h_i = Z_{ij}^h \rho_j$ . We identify  $h_1$  as the 125 GeV Higgs boson observed at the experiments and treat  $h_2$  as the singlet dominated scalar. The other scalars (belonging primarily to the  $H_2$  doublet) are taken to be degenerate in mass and very heavy ( $> 3$  TeV). We shall work in the limit  $\tan \beta = v_2/v_1 < 10^{-3}$  such that the only relevant admixture in  $h_1$  is from the singlet scalar which is parametrised by the mixing component  $Z_{13}^h$ .

A non-zero VEV to  $H_2$  charged under  $U(1)_X$  allows a mixing between  $Z$  and  $Z'$ . Note that the presence of  $H_2$  and its participation in the symmetry breaking mechanism is crucial in giving mass to light neutrinos and generate the correct mixings in the neutrino sector [14]. We show in Eq. (3) the resulting  $Z$ - $Z'$  mixing angle as a function of the gauge couplings and VEVs [14],

$$\tan 2\theta' = \frac{2g_z (g'_x v^2 + 2g_x v_2^2)}{g'^2_x v^2 + 4g_x g'_x v_2^2 + 4g_x^2 (v_2^2 + 4v_s^2) - g_z^2 v^2}, \tag{3}$$

where  $v = \sqrt{v_1^2 + v_2^2} \simeq 246$  GeV,  $g_z = \sqrt{g_1^2 + g_2^2}$  and  $g'_x$  measures the strength of gauge kinetic mixing. A desirable and natural choice for  $Z$ - $Z'$  mixing angle would be to choose it smaller, such that it does not modify the  $Z$  boson couplings with the SM fields. Precision data from LEP experiments on the  $Z$  boson properties put an upper bound of  $10^{-3}$  on  $\theta'$  [19]. The small value for  $\theta'$  consistent with the LEP constraints can be easily achieved with  $\tan \beta < 10^{-3}$  and  $g'_x \simeq 0$ , avoiding the need to fine-tune  $g_x$  to any unnatural value. We must note that kinetic mixing is unavoidable and will be generated at one-loop since  $H_2$  is charged under both  $U(1)_Y$  and  $U(1)_X$ . However in a UV complete set-up it is possible to cancel the one-loop contribution to the kinetic mixing by introducing additional fields without affecting the phenomenology of the model [20]. Such cancellations can help in obtaining much smaller values of  $g'_x$ , and the small GKM will make the  $Z'$  interact very weakly with all SM matter fields, making it practically invisible and very difficult to observe. This would be akin to the situation we faced in our search for the SM Higgs boson which coupled very weakly to the light fermions and made it very difficult to discover the (now observed) SM Higgs boson at LEP and Tevatron. The main highlight of this work is to show the discovery channels for this invisible mediator and the importance of the Higgs sector of the model in producing

<sup>1</sup> We ignore the possibility of generating neutrino mass radiatively in this study.

<sup>2</sup> This term can be generated dynamically by adding new scalars to the model.

| $\lambda_1$ | $\lambda_s$ | $\lambda_2$ | $\lambda_{12}$ | $\lambda'_{12}$ | $\lambda_{2s}$ | $\mu_{12}$<br>(GeV <sup>2</sup> ) | $v_s$<br>(GeV) | $\tan \beta$ |
|-------------|-------------|-------------|----------------|-----------------|----------------|-----------------------------------|----------------|--------------|
| 0.12875     | 1.044       | 1.0         | 0.005          | 0.005           | 0.0            | $10^3$                            | 100            | $10^{-4}$    |

TABLE II. Scalar sector parameters consistent with all experimental constraints, where  $(m_{h_1}, m_{h_2}) = (125, 144.5)$  GeV.

the otherwise hidden  $Z'$ . We therefore work in the limit of small GKM and  $\tan \beta$  values which help in avoiding strong limits on the  $Z'$  mass and the gauge coupling  $g_x$  [14], and leads to interesting signals for  $Z'$  decay.

We now focus on the limits that may arise from the Higgs sector. Note that the scalars belonging to the second Higgs doublet are very heavy and satisfy the constraints trivially. The constraints on the remaining scalars and their mixing is established using the publicly available packages **HiggsBounds** [22, 23] and **HiggsSignals** [21]. These tools check for theoretical constraints on the Higgs mass as well as exclusions using the observed signal strength for the Higgs boson from LHC experiments. The experimental values are compared with expected deviations that may arise in any extended scalar sector which modifies the Higgs composition and its couplings. This allows us to obtain values for parameters in the Lagrangian which would be compatible with the observed Higgs boson and its decay probabilities [24, 25] in our model. More details of the constraints on the model parameters is given in our earlier work [14].

Another interesting observation that we must highlight in our minimal model is the possibility to accommodate a DM candidate. We have three singlet left and right-handed neutrinos in the model and one of them becomes the DM if we appropriately choose one of the Yukawa couplings  $Y_{\nu_{ij}}$  (shown in Eq. (1)) to be very small. We find that a pair of heavy neutrinos ( $\nu_4$  and  $\nu_5$ ), degenerate in mass get a decay lifetime larger than the age of the Universe for  $Y_{\nu_{11}} \lesssim 10^{-27}$ <sup>3</sup> and  $Y_{\nu_{1j}} = Y_{\nu_{j1}} = 0$ . This choice however makes the DM coupling to any of the SM states very weak, leading to the unwanted scenario of an overabundant DM in the Universe. The viability of DM being a thermal relic with the correct relic density is re-enforced if the particle spectrum has non-SM lighter states to which the DM couples strongly enough, such that it can annihilate into these. This motivates us to choose the singlet scalar and  $Z'$  lighter than the fermionic DM candidates ( $\nu_4$  and  $\nu_5$ ). The dominant annihilation channels for the DM then become  $\nu_4 \nu_5 \rightarrow h_2 Z'$  ( $t$ -channel via  $\nu_4$  and  $\nu_5$ ),  $\nu_4 \nu_4 \rightarrow Z' Z' (h_2 h_2)$ ,  $\nu_5 \nu_5 \rightarrow Z' Z' (h_2 h_2)$ , where  $h_2$  is the singlet  $S$  dominated scalar. Here all interactions proceed via the unsuppressed  $g_x$  coupling strength.

The light  $Z'$  and  $h_2$  which facilitate the DM to be a thermal relic can be observed at the LHC through the

Higgs mediated channel. To show how such a signal can be observed at the LHC and the simultaneous possibility of the DM relic being satisfied, we fix the scalar sector by choosing  $h_1$  to be SM-like with mass  $m_{h_1} \simeq 125$  GeV and keep the singlet  $S$  dominated  $h_2$  mass  $m_{h_2} \simeq 144.5$  GeV, while the others are very heavy. We choose the fixed values in Table II since any other choice will not give any new characteristic features and only affect the overall production rate (through  $v_s$ ). The most relevant parameters in our analysis become the gauge coupling  $g_x$

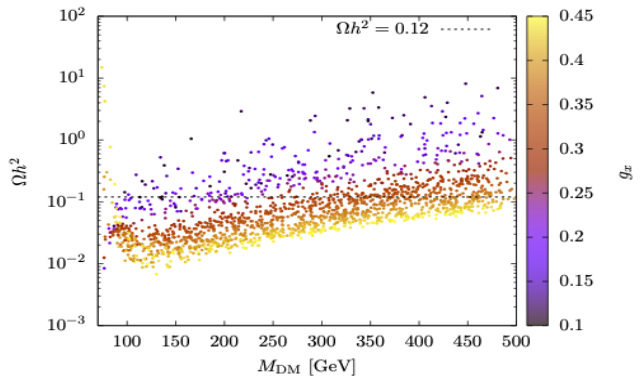


FIG. 1. The relic density  $\Omega h^2$  as a function of the DM mass and the gauge coupling  $g_x$ .

that affects the  $Z'$  mass and its coupling, and the quartic coupling  $\lambda_{1s}$  which would affect the scalar sector mixing between the  $H_1$  and  $S$  components. We therefore scan over only these parameters and fix the other parameters of the model. Note that varying  $\lambda_{1s}$  would also vary the  $h_1$  and  $h_2$  masses and is constrained to be  $< 0.033$  at the  $3\sigma$  level by the measured Higgs boson mass of  $125.25 \pm 0.17$  GeV [19]. This constrains the  $h_2$  mass to be in the range 144.5-145 GeV. We show the DM relic density in Fig. 1 for the choice of parameter values and the scalar masses shown in Table II. Quite clearly we can find a wide range of values for the DM in the model to satisfy the relic density requirements of  $\Omega h^2 = 0.120 \pm 0.001$  at 90% CL [26]. The points are also allowed by XENON1T and PandaX-4T [27–29] constraints on both spin-independent (SI) and spin-dependent (SD) direct detection cross sections. They also align with the indirect detection (annihilation of the DM pair to SM particles that could produce distinctive signatures in cosmic rays) constraints coming from the FERMI-LAT [30], MAGIC [31] and PLANCK [26] experiments in the given range due to the suppressed couplings with SM particles. The compatible points which give the correct relic density are found to have a typical DM-neutron cross section of  $\lesssim 10^{-47}$  cm<sup>2</sup>. We must however point out that the choice of parameters is not limited and the above is simply an example to show how easily a DM candidate could be accommodated in the model. As we show later, this can also play a crucial role for the LHC signal of  $Z'$ . A much more detailed DM analysis involving the full

<sup>3</sup> This provides an upper bound on the coupling strength and could also be chosen zero.

scan of the model parameter space is left for future work [32].

We are now ready to analyse the light  $Z'$  signal at the LHC based on the choice of parameters given in Table II. Note that the mixing  $Z_{13}^h$  plays a crucial role in the pair production of  $Z'$  at the LHC via scalar mediators. With this mixing the scalar mediator can be produced via gluon-gluon fusion and will subsequently decay to a  $Z'$  pair due to the gauge coupling  $g_x$ , giving us a unique opportunity to study the otherwise weakly coupled  $Z'$  boson. The value of the mixing parameter  $Z_{13}^h$  determines the cross section of this process. The  $Z'$  would easily evade direct searches for very small values of GKM and  $\tan\beta$ . As the SM particle couplings with  $Z'$  are proportional to  $\theta'$ , the direct production of  $Z'$  via fermion interaction is negligible for our chosen value of  $g'_x$  and  $\tan\beta$ . The scalar responsible for giving a mass to the  $Z'$  therefore becomes the mediator which eventually helps in its production and its detection at experiments. We focus on the process

$$pp \rightarrow h_{1,2} \rightarrow Z' Z',$$

and show the  $Z'$  pair production cross section at the LHC in Fig. 2 for different values of the mixing parameter  $Z_{13}^h$ . As expected, larger values of the mixing lead to significant production cross sections which could give clear hints of the  $Z'$ . The mixing  $Z_{13}^h$  also affects the observed Higgs boson production and decay and is therefore constrained by Higgs boson measurements at LHC. We can estimate the valid region of our signal cross section by scanning over the light  $Z'$  mass ( $70 \text{ GeV} > M_{Z'} > 20 \text{ GeV}$ ) and the mixing parameter ( $0.12 > |Z_{13}^h| > 0$ ) in the Higgs sector. The scan checks for the variation of Higgs signal strengths in the observed final states within allowed experimental bands at 95% C.L. and also uses a requirement on the allowed deviations in the Higgs branching to new modes to be less than 13% (including invisible Higgs boson decays [33]). This gives us a corresponding upper bound on  $Z'$  pair production via the Higgs mediators, which is highlighted as the hatched region obtained using **HiggsSignals**. The SM-like  $h_1$  is the major contributor to  $Z'$  production when  $M_{Z'} \leq m_{h_1}/2$ , while the singlet-dominated  $h_2$  becomes the dominant contributor beyond this mass range. Note that the contribution from the singlet dominated  $h_2$  is more or less constant for  $M_{Z'} \leq m_{h_2}/2$  since the decay branching fraction of  $h_2 \rightarrow Z' Z'$  is 100%, a very specific feature of this model different from other  $U(1)$  extensions considered in the literature. The off-shell contributions to the production fall rapidly for both  $h_1$  and  $h_2$  as is evident from Fig. 2. In the region  $m_{h_2}/2 > M_{Z'} > 62.5 \text{ GeV}$ , an increase in  $Z' Z'$  production is only achieved through an increase in  $h_2$  production and, correspondingly, an increase in  $Z_{13}^h$ . This parameter is constrained by the observed signal strengths of the 125 GeV Higgs boson, so the total cross section in this region is also con-

strained to be small (see the hashed **HiggsSignal** zone in Fig. 2).

We however underline the importance of the above production channels as these might be the only relevant modes of observation of a light  $Z'$  characterizing a *hidden gauge symmetry*.

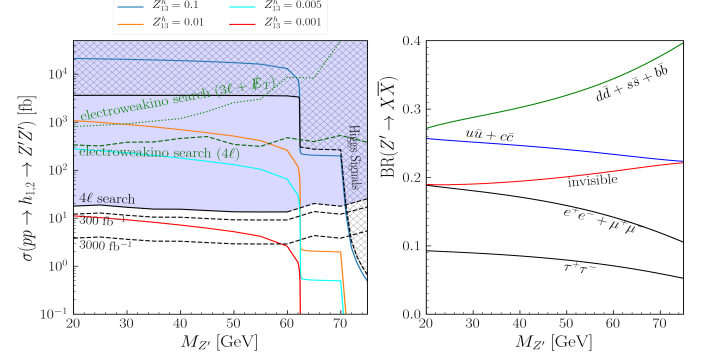


FIG. 2. The pair production cross section of  $Z'$  at the LHC via  $h_1$  and  $h_2$  and its tree-level decay branching ratios along with current limits.

The constraints on the production cross section do not significantly affect the decay, as the sub-100 GeV  $Z'$  has a small total decay width,  $\Gamma_{Z'} \sim \mathcal{O}(10^{-9} - 10^{-8}) \text{ GeV}$  but decays promptly (within the detector). The branching ratios for  $Z'$  decay are shown in Fig. 2. Using the parameter space of Fig. 2 as representative points for the model we highlight the prospect of observing the  $Z'$  signal at the LHC in its most sensitive  $4\ell$  channel, where  $\ell = e, \mu$ . Although the  $4\ell$  channel is the most likely channel of observing  $Z'$  signal, other final states comprising of leptons and jets could also manifest as the channels of discovery. This implies that a multi-channel final state can constrain the parameter space of the model. Many searches extending over different multi-channel final states have been carried out by experiments at LHC in the context of different BSM models. It is therefore natural to put our parameter region to test by determining the expected signal yields in search channels constrained by the LHC experiments. A popular public code called **CheckMATE** [34] is used by the high-energy community to obtain limits on new BSM models from such experimental searches. We obtain a weak bound from **CheckMATE** which arises mainly from the multi-lepton searches for supersymmetric electroweakinos [35]. In the aforementioned search, different signal regions are identified based on the supersymmetric mass spectrum. The basic selection criteria employed for jets and leptons are:  $p_{T_j} > 25 \text{ GeV}$  and  $p_{T_\ell} > 10 \text{ GeV}$  with the same rapidity coverage of  $|\eta| < 2.4$ . The leptons and jets are isolated by  $\Delta R_{j\ell} > 0.4$  and events with at least one b-jet are vetoed [35]. The dominant channel contributing to a bound for our parameter space comes from the  $4\ell$  final state as the  $Z'$  can decay to electrons and muons combined with a probability of 18% to 20%. The  $4\ell$  sig-



| Search Channel         | Signal Region | Kinematic Selection (GeV)  |
|------------------------|---------------|--|
| $3\ell + \cancel{E}_T$ | A01           | $p_{T_{e(\mu)_1}} > 25(20), p_{T_{e(\mu)_2}} > 15(10), m_{\ell-\ell^+} < 75, M_T < 100, \cancel{E}_T : (50 - 100)$             |
| $4\ell$                | (G01,G02,G03) | $p_{T_{e(\mu)_1}} > 25(20), p_{T_{e(\mu)_2}} > 15(10), m_{\ell-\ell^+} < 75, \cancel{E}_T : (0 - 50), (50 - 100), (100 - 150)$ |

TABLE III. Kinematic selection and various signal regions in the  $3\ell + \cancel{E}_T$  and  $4\ell$  channels in Electroweakino searches at CMS [35]. The subleading leptons must satisfy  $p_{T_{e(\mu)}} > 15(10)$  GeV. If the leading lepton is a muon and the other leptons are electrons, the muon threshold is increased to  $p_T > 25$  GeV. Signal acceptance for the  $3\ell + \cancel{E}_T$  ( $4\ell$ ) channel is around 5.3% (17%) for  $M_{Z'} = 25$  GeV and around 2.6% (29%) for  $M_{Z'} = 50$  GeV, respectively.

nal regions in Ref. [35] are categorised using kinematic windows of  $\cancel{E}_T$  as G01, G02 and G03. Their kinematic selection is listed in Table III and the relevant constraint is shown in Fig. 2 as *electroweakino search* ( $4\ell$ ). Note that the  $Z'$  in our study is light and therefore the jets and leptons from its decay will have low  $p_T$ . Hence some of the soft leptons may not satisfy the selection criteria. For a  $Z'$  boson mass less than 50 GeV, a larger fraction of events in  $Z'Z' \rightarrow 4\ell$  do not satisfy the selection criteria  $p_{T_\ell} > 10$  GeV for all leptons. We find that the signal region A01 in Ref. [35] provides the strongest constraint in the  $3\ell + \cancel{E}_T$  channel. We expect this constraint to be a bit stronger for lower  $M_{Z'}$  values, whereas above 50 GeV of  $M_{Z'}$  the constraint from  $3\ell + \cancel{E}_T$  will get weaker. Note that the signal in our model will not have large  $\cancel{E}_T$ . So the exclusion cut of  $\cancel{E}_T < 50$  GeV as defined in CMS analysis on  $3\ell + \cancel{E}_T$  reduces its sensitivity significantly, as seen in Fig. 2. The above bounds come from the direct search and are expectedly stronger than the HiggsSignal bounds for  $M_{Z'} < 62.5$  GeV, as shown by the corresponding *electroweakino search* exclusion curves in Fig. 2.

The most relevant and strongest bound however comes from a  $4\ell$  signal which was recently looked at by ATLAS [36]. The analysis gives a differential cross section measurement of the 4 lepton final state in the SM. This also happens to be the discovery channel for our  $Z'$  and one expects to see resonant bumps in the dilepton invariant mass distributions. We can therefore use this analysis directly to test for hints of a  $Z'$  boson. The ATLAS analysis has been included in the Rivet-3.1.4 [37, 38] package, allowing a direct comparison of the experimental result with predictions of our signal. We include our model output for the aforementioned final state and use the package Contur [39] to evaluate robust limits on the parameter space shown in Fig. 2. To put the bounds in perspective we note that in the  $h_1 \rightarrow 4\ell$  signal region applicable to  $20 \text{ GeV} \leq M_{Z'} \leq 62.5 \text{ GeV}$ , the dilepton invariant mass variable  $m_{34}$ <sup>4</sup> (Fig 7b) in Ref. [36] has a larger bin wise SM cross section than  $m_{12}$  (Fig 6b) in the  $0 - 60$  GeV bin. This is expected as the second pair of leptons arise from an off-shell  $Z$  in the SM background events. Although  $m_{12}$  has a coarser bin in  $0 - 50$  GeV,

most of the SM events have values of this variable near the  $Z$  peak, and the total cross section in the  $0 - 50$  GeV bin is  $\mathcal{O}(10^{-2})$  fb. Hence  $m_{12}$  constrains our parameter space most because our model results in a  $Z'$  peak in this region. For  $M_{Z'} > 62.5$  GeV the relevant measurement region is  $m_{h_1}/2 < m_{4\ell} < m_{h_2}/2$  [36] in our analysis, where the SM predicts the first and the second lepton pairs to come from on-shell and off-shell  $Z$  bosons, respectively. Hence the second lepton pair invariant mass  $m_{34}$  distribution gives a tail above 60 GeV, whereas for  $m_{12}$  the cross section above 60 GeV is higher compared to  $m_{34}$  due to the presence of the SM  $Z$  peak. In our model the relevant  $Z'$  boson mass range is  $75 > M_{Z'} > 62.5$  GeV and we expect a stronger constraint from  $m_{34}$  where the SM background yields are smaller. The other kinematic variables including the full  $4\ell$  invariant mass give weaker limits as the bin wise background cross section is much higher than in the relevant bins of the dilepton invariant mass, but the  $4\ell$  invariant mass contributes in the final *chi-square* fit of Contur. Note the specific bumps in the exclusion plots at  $M_{Z'} \simeq 62, 72$  GeV where the sensitivity decreases suddenly. These points correspond to kinematic thresholds where  $h_{1,2} \rightarrow Z'Z'$  become off-shell, leading to drop in signal yields. The measurement strategy in the ATLAS analysis employs 50 distributions in kinematic variables which can be also used to propose search sensitivity for our hypothesized  $Z'$  boson for given values of  $Z'_{13}$  for high integrated luminosity options of the LHC. We show in Fig. 2, the sensitivity curves with  $300 \text{ fb}^{-1}$  and  $3000 \text{ fb}^{-1}$  integrated luminosity at the LHC, assuming a rather pessimistic view that similar efficiencies of the 13 TeV analysis could be applicable to the 14 TeV run. The events for the analysis were generated using MadGraph5@aMCNLO [40, 41] and showered using Pythia 8 [42]. The HepMC [43] output was then included in Rivet [37, 38] and run for the ATLAS analysis of Ref. [36]. The resulting YODA file was then input to Contur [39, 44] to evaluate a likelihood fit and determine the exclusions on the model parameter space. We propose that  $h_1 \rightarrow 4\ell$  is the most sensitive channel to search for a light  $Z'$  symbolising a hidden symmetry that couples weakly to SM particles and can lie hidden in the LHC data.

We now comment on some interesting possibilities for our model which can have a major impact on the search strategies for the  $Z'$  boson when radiative decays of the

<sup>4</sup> Subscripts represent the  $p_T$  ordered lepton numbers.

| $Z'$ decay   | $\sum \nu_a \nu_b$ | $\sum \ell_a^+ \ell_a^-$ | $\sum \ell_a^\pm \ell_b^\mp$ | $\sum j j$    | $\Gamma_{Z'} \text{ (GeV)}$ |
|--|--------------------|--------------------------|------------------------------|---------------|-----------------------------|
| $Y_{\nu_{ij}}^{i \neq j} = 0, Y_{\nu}^{ii} \simeq 10^{-3}$     | $0.23 (10^{-3})$   | $0.16 (10^{-4})$         | $0 (10^{-4})$                | $0.61 (0)$    | $2 \times 10^{-9}$          |
| $Y_{\nu_{ij}}^{i \neq j} \simeq 0.32, Y_{\nu}^{ii} \simeq 0.8$ | $10^{-3} (0.50)$   | $10^{-3} (0.340)$        | $0 (0.16)$                   | $10^{-3} (0)$ | $1.130 \times 10^{-6}$      |

TABLE IV. Decay probabilities of  $Z'$  at tree-level (one-loop) for different  $Y_{\nu_{ij}}$ . Here  $\ell_a = \mu, \tau$ , and  $M_{Z'} = 60 \text{ GeV}$ ,  $g_x = 0.3$ ,  $Y_{\nu}^{11} = 0$  and  $Y_{\nu}^{1j} = 0$  with  $\theta' \simeq 10^{-5}$ .

$Z'$  boson become very important. The term  $Y_{\nu} \bar{l}_L H_2 N_R$  in the Lagrangian determines how large the radiative decay is. We find that for  $Y_{\nu} \sim 10^{-1}$  the loop induced decays shown in Fig. 3 have amplitudes which are proportional to  $Y_{\nu}^2$  and start becoming comparable to the tree-level modes driven by  $Z$ - $Z'$  mixing. An immediate and interesting consequence of this result is that the  $Z'$  boson behaves as a leptophilic boson with no decay to quarks. Note that the mixing of the light neutrino with heavy neutrinos is still very small unlike the typical inverse-seesaw mechanism, due to the choice of very small  $\tan \beta$  values. We evaluate the one-loop decays of the  $Z'$

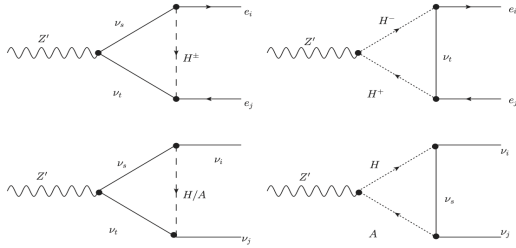


FIG. 3. Feynman diagrams for the one-loop decays of the  $Z'$  boson to neutrinos and charged leptons.

boson and show a comparison of the decay branching ratios in Table IV for two choices of the Yukawa couplings. The loop diagrams have been calculated analytically with the help of **Package-X** [48] and numerical results were obtained with the help of **LoopTools** [49]. The branching fraction of the  $Z'$  boson to the exotic LFV modes could be arranged at the level of 15 – 25% by suitably varying the  $Y_{\nu}$  values. In a likely scenario of radiative decays dominating, the  $Z'$  boson decays dominantly (50%) to light neutrinos contributing to the invisible decay mode of the Higgs when  $M_{Z'} \leq m_{h_1}/2$ . The invisible mode would render the search for such a  $Z'$  at the LHC very challenging. The most likely place of discovery in such a scenario would be at future lepton colliders. The leptophilic nature also leads to an increase in the charged lepton decay branching fraction of the  $Z'$  boson to 50%, giving a stronger limit than what is obtained in Fig. 2. In addition, it opens up a more interesting possibility of observing LFV decays of the  $Z'$  in the  $h_1 \rightarrow 4\ell$  signal [45–47]. The ATLAS analysis [36] only looks at the invariant mass distributions of opposite-sign-same-flavour leptons

while in our case we will have a substantial decay mode of  $Z' \rightarrow e\mu$  which will show up as an invariant mass peak in the wrong flavour mode (see Fig. 4). We find that an

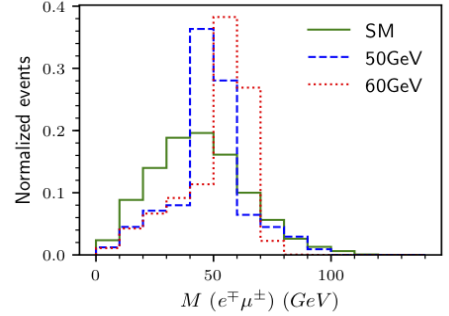


FIG. 4. Illustrating the invariant mass peaks in the wrong flavour mode, due to one-loop decay of the  $Z'$  boson.

improvement of up to 60% is achieved for signal sensitivity when this variable is included in the analysis. This would therefore provide a clear new signal and huge improvement over the existing search for our model. A more unique possibility with very little SM background arises if we consider only the LFV decay of  $Z' \rightarrow e^\mp \mu^\pm$ . This would give two pairs of same-flavour-same sign charged leptons.

These LFV modes of the  $Z'$  boson could then clearly be observed at the LHC by focusing on the LFV searches in the Higgs decay which are of great current interest [50]. A more promising search scenario would be in machines vouched as Higgs factories [51–54] where the  $h_1 \rightarrow Z' Z'$  mode can be looked at with more precision. A close examination of the parameter space that could lead to such possibilities is interesting but beyond the scope of this work, and we leave it for future studies.

To conclude, we have highlighted through this Letter how a light  $Z'$  in a popular and well motivated  $U(1)$  extension of the SM can easily stay hidden in the LHC data if the new symmetry does not speak to the SM sector directly. We motivate such a scenario through the neutrino sector by introducing a neutrinophilic  $U(1)$  which can also provide a DM candidate. The weakly interacting DM candidate gives the correct relic density when the  $Z'$  boson is lighter than the DM candidate. We then highlight how such a light  $Z'$  can be produced at the LHC via the Higgs channel. The existing LHC searches for such modes in the Higgs channel could be sensitive to a significant parameter space of our model which is explicitly

shown by considering independent search channels and analyzing their effect on our parameter space. A very interesting consequence of the model is the decay of the  $Z'$  boson via a loop when it does not directly couple with SM fields, giving the possibility of it being a leptophilic gauge boson. The typically non-diagonal mixing in the light and heavy neutrino states and the structure of the  $Y_\nu$  Yukawa coupling matrix can lead to LFV decays of  $Z'$  which will open up more interesting signatures of the model at the LHC and future lepton colliders.

The authors would like to acknowledge support from the Department of Atomic Energy, Government of India, for the Regional Centre for Accelerator-based Particle Physics (RECAPP).

---

\* awaleed@sci.cu.edu.eg

† anjanbarik@hri.res.in

‡ skrai@hri.res.in

§ tousiksamui@hri.res.in

- [1] G. Aad et al. (ATLAS), *Phys. Lett. B* **716**, 1 (2012), [arXiv:1207.7214 \[hep-ex\]](#).
- [2] S. Chatrchyan et al. (CMS), *Phys. Lett. B* **716**, 30 (2012), [arXiv:1207.7235 \[hep-ex\]](#).
- [3] J.-h. Kang, P. Langacker, and T.-j. Li, *Phys. Rev. D* **71**, 015012 (2005), [arXiv:hep-ph/0411404](#).
- [4] E. Ma, *Phys. Lett. B* **380**, 286 (1996), [arXiv:hep-ph/9507348](#).
- [5] V. Barger, C. Kao, P. Langacker, and H.-S. Lee, *Phys. Lett. B* **600**, 104 (2004), [arXiv:hep-ph/0408120](#).
- [6] B. de Carlos and J. R. Espinosa, *Phys. Lett. B* **407**, 12 (1997), [arXiv:hep-ph/9705315](#).
- [7] S. W. Ham and S. K. OH, *Phys. Rev. D* **76**, 095018 (2007), [arXiv:0708.1785 \[hep-ph\]](#).
- [8] M. Cvetič, D. A. Demir, J. R. Espinosa, L. L. Everett, and P. Langacker, *Phys. Rev. D* **56**, 2861 (1997), [Erratum: *Phys.Rev.D* 58, 119905 (1998)], [arXiv:hep-ph/9703317](#).
- [9] P. Langacker and M. Plumacher, *Phys. Rev. D* **62**, 013006 (2000), [arXiv:hep-ph/0001204](#).
- [10] P. Langacker, G. Paz, L.-T. Wang, and I. Yavin, *Phys. Rev. Lett.* **100**, 041802 (2008), [arXiv:0710.1632 \[hep-ph\]](#).
- [11] J. Kang, P. Langacker, T. Li, and T. Liu, *JHEP* **04**, 097 (2011), [arXiv:0911.2939 \[hep-ph\]](#).
- [12] P. Langacker, *Rev. Mod. Phys.* **81**, 1199 (2009), [arXiv:0801.1345 \[hep-ph\]](#).
- [13] E. Accomando, D. Becciolini, A. Belyaev, S. De Curtis, D. Dominici, S. F. King, S. Moretti, and C. Shepherd-Themistocleous, *PoS DIS2013*, 125 (2013).
- [14] W. Abdallah, A. K. Barik, S. K. Rai, and T. Samui, *Phys. Rev. D* **104**, 095031 (2021), [arXiv:2106.01362 \[hep-ph\]](#).
- [15] M. Berbig, S. Jana, and A. Trautner, *Phys. Rev. D* **102**, 115008 (2020), [arXiv:2004.13039 \[hep-ph\]](#).
- [16] E. Accomando, L. Delle Rose, S. Moretti, E. Olaiya, and C. H. Shepherd-Themistocleous, *JHEP* **02**, 109 (2018), [arXiv:1708.03650 \[hep-ph\]](#).
- [17] S. Amrith, J. M. Butterworth, F. F. Deppisch, W. Liu, A. Varma, and D. Yallup, *JHEP* **05**, 154 (2019), [arXiv:1811.11452 \[hep-ph\]](#).
- [18] K. Das, T. Li, S. Nandi, and S. K. Rai, *Eur. Phys. J. C* **78**, 35 (2018), [arXiv:1708.00328 \[hep-ph\]](#).
- [19] P. A. Zyla et al. (Particle Data Group), *PTEP* **2020**, 083C01 (2020).
- [20] F. del Aguila, M. Masip, and M. Perez-Victoria, *Nucl. Phys. B* **456**, 531 (1995), [arXiv:hep-ph/9507455](#).
- [21] P. Bechtel, S. Heinemeyer, O. Stål, T. Stefaniak, and G. Weiglein, *Eur. Phys. J. C* **74**, 2711 (2014), [arXiv:1305.1933 \[hep-ph\]](#).
- [22] P. Bechtel, O. Brein, S. Heinemeyer, G. Weiglein, and K. E. Williams, *Comput. Phys. Commun.* **181**, 138 (2010), [arXiv:0811.4169 \[hep-ph\]](#).
- [23] P. Bechtel, O. Brein, S. Heinemeyer, G. Weiglein, and K. E. Williams, *Comput. Phys. Commun.* **182**, 2605 (2011), [arXiv:1102.1898 \[hep-ph\]](#).
- [24] G. Aad et al. (ATLAS, CMS), *JHEP* **08**, 045 (2016), [arXiv:1606.02266 \[hep-ex\]](#).
- [25] A. Sopczak (ATLAS, CMS), *PoS FFK2019*, 006 (2020), [arXiv:2001.05927 \[hep-ex\]](#).
- [26] N. Aghanim et al. (Planck), *Astron. Astrophys.* **641**, A6 (2020), [Erratum: *Astron.Astrophys.* 652, C4 (2021)], [arXiv:1807.06209 \[astro-ph.CO\]](#).
- [27] E. Aprile et al. (XENON), *Phys. Rev. Lett.* **121**, 111302 (2018), [arXiv:1805.12562 \[astro-ph.CO\]](#).
- [28] E. Aprile et al. (XENON), *Phys. Rev. Lett.* **122**, 141301 (2019), [arXiv:1902.03234 \[astro-ph.CO\]](#).
- [29] Y. Meng et al. (PandaX-4T), (2021), [arXiv:2107.13438 \[hep-ex\]](#).
- [30] T. Daylan, D. P. Finkbeiner, D. Hooper, T. Linden, S. K. N. Portillo, N. L. Rodd, and T. R. Slatyer, *Phys. Dark Univ.* **12**, 1 (2016), [arXiv:1402.6703 \[astro-ph.HE\]](#).
- [31] M. L. Ahnen et al. (MAGIC, Fermi-LAT), *JCAP* **02**, 039 (2016), [arXiv:1601.06590 \[astro-ph.HE\]](#).
- [32] W. Abdallah, A. K. Barik, S. K. Rai, and T. Samui, Work in Progress (2021).
- [33] M. Aaboud et al. (ATLAS), *Phys. Lett. B* **793**, 499 (2019), [arXiv:1809.06682 \[hep-ex\]](#).
- [34] M. Drees, H. Dreiner, D. Schmeier, J. Tattersall, and J. S. Kim, *Comput. Phys. Commun.* **187**, 227 (2015), [arXiv:1312.2591 \[hep-ph\]](#).
- [35] A. M. Sirunyan et al. (CMS), *JHEP* **03**, 166 (2018), [arXiv:1709.05406 \[hep-ex\]](#).
- [36] G. Aad et al. (ATLAS), *JHEP* **07**, 005 (2021), [arXiv:2103.01918 \[hep-ex\]](#).
- [37] A. Buckley, J. Butterworth, D. Grellscheid, H. Hoeth, L. Lonnblad, J. Monk, H. Schulz, and F. Siegert, *Comput. Phys. Commun.* **184**, 2803 (2013), [arXiv:1003.0694 \[hep-ph\]](#).
- [38] C. Bierlich et al., *SciPost Phys.* **8**, 026 (2020), [arXiv:1912.05451 \[hep-ph\]](#).
- [39] A. Buckley et al., *SciPost Phys. Core* **4**, 013 (2021), [arXiv:2102.04377 \[hep-ph\]](#).
- [40] J. Alwall, M. Herquet, F. Maltoni, O. Mattelaer, and T. Stelzer, *JHEP* **06**, 128 (2011), [arXiv:1106.0522 \[hep-ph\]](#).
- [41] J. Alwall, R. Frederix, S. Frixione, V. Hirschi, F. Maltoni, O. Mattelaer, H. S. Shao, T. Stelzer, P. Torrielli, and M. Zaro, *JHEP* **07**, 079 (2014), [arXiv:1405.0301 \[hep-ph\]](#).
- [42] T. Sjöstrand, S. Ask, J. R. Christiansen, R. Corke, N. Desai, P. Ilten, S. Mrenna, S. Prestel, C. O. Rasmussen, and P. Z. Skands, *Comput. Phys. Commun.* **191**, 159 (2015), [arXiv:1410.3012 \[hep-ph\]](#).

- [43] M. Dobbs and J. B. Hansen, [ATL-SOFT-2000-001](#), Tech. Rep. (CERN, Geneva, 2000).
- [44] J. M. Butterworth, D. Grellscheid, M. Krämer, B. Sarrazin, and D. Yallup, *JHEP* **03**, 078 (2017), [arXiv:1606.05296 \[hep-ph\]](#).
- [45] J. G. Korner, A. Pilaftsis, and K. Schilcher, *Phys. Lett. B* **300**, 381 (1993), [arXiv:hep-ph/9301290](#).
- [46] M. J. Herrero, X. Marcano, R. Morales, and A. Szykman, *Eur. Phys. J. C* **78**, 815 (2018), [arXiv:1807.01698 \[hep-ph\]](#).
- [47] V. Brdar, M. Lindner, S. Vogl, and X.-J. Xu, *Phys. Rev. D* **101**, 115001 (2020), [arXiv:2003.05339 \[hep-ph\]](#).
- [48] H. H. Patel, *Comput. Phys. Commun.* **197**, 276 (2015), [arXiv:1503.01469 \[hep-ph\]](#).
- [49] T. Hahn and M. Perez-Victoria, *Comput. Phys. Commun.* **118**, 153 (1999), [arXiv:hep-ph/9807565](#).
- [50] A. M. Sirunyan et al. (CMS), *JHEP* **06**, 001 (2018), [arXiv:1712.07173 \[hep-ex\]](#).
- [51] P. Bambade et al., (2019), [arXiv:1903.01629 \[hep-ex\]](#).
- [52] M. Dong et al. (CEPC Study Group), (2018), [arXiv:1811.10545 \[hep-ex\]](#).
- [53] A. Abada et al. (FCC), *Eur. Phys. J. ST* **228**, 261 (2019).
- [54] L. Calibbi, X. Marcano, and J. Roy, (2021), [arXiv:2107.10273 \[hep-ph\]](#).